SLAC-PUB-1894
PEP-228A
LBL-6163
March 1977
(A)

BUNCH LENGTHENING AND RELATED EFFECTS IN SPEAR II*

P. B. Wilson, R. Servranckx,† A. P. Sabersky,
J. Gareyte,†† G. E. Fischer, A. W. Chao

Stanford Linear Accelerator Center
Stanford University, Stanford, California 94305

M.H.R. Donald

Lawrence Berkeley Laboratory
University of California, Berkeley, California 94720

Introduction

In recent years, electron storage ring designers have become aware of the problems caused by the interaction of short, high current bunches with their environment. Important effects are: (1) energy loss can cause local overheating of chamber components; (2) additional RF power is required due to overall energy loss; (3) the increased energy spread requires increased aperture; (4) destructive instabilities could occur. In the following work, anomalous bunch lengthening and energy spread, the spectroscopy of longitudinal modes and the shift of synchronous phase have been simultaneously measured in order to study the dynamics of the interaction. From the data obtained at SPEAR II one is led to a model of coupling impedance which should be useful in the design of any electron ring.

Instrumentation, Method of Data Aquisition, and Measurement Errors

Bunch Lengthening

Visible synchrotron light is brought out through the ring shielding and is focused on a high speed photodiode (ITL HSD50), directly coupled to the sampling head (hp-1870A) of an oscilloscope (hp-1815A), which is triggered by a delayed beam-derived signal. The output is read by a digital signal averager which permits measurement of signals otherwise below the noise level. Signals from single bunches as low as 0.2 mA in average current can thus be measured. The entire system is checked for linearity by placing optical filters in front of the diode. Time calibration is obtained by axially displacing the diode a known distance. A simple physical model of the diode response function yields a second moment $\sigma = 60$ ps $\pm$ 10%, consistent with the value derived from the data. Bunch traces are recorded on an X-Y plotter; the FWHM is measured by hand and corrected for the diode response to obtain σ_z. As in SPEAR I,[1] the bunch shapes show marked asymmetry, which leads one to consider analyzing the higher moments of the bunches via more elaborate techniques. However, these measures are meaningful only if the data is free from equipment-caused distortions, e.g., ringing and base line shift. It may be possible in the future, after a direct measurement of the impulse response of the apparatus, to obtain more accurate bunch shapes by deconvolution. The measurement error is dominated by uncertainties in calibration and trace measurement and is estimated to be ~4% on the average. Values of σ_z are then divided by σ_{z0} (for constant ν_s), calculated from machine parameters in the classical way.[2]

Energy Spread (Core)

The horizontal profile of the beam, derived from the optical scanning system[3] and integrated by a box-car integrator, is measured at a point in the lattice having sufficient energy dispersion (η) to separate synchrotron from betatron amplitudes. The major sources of error derive from imperfect knowledge of the η and β functions at the monitored point and the exact linearity of the optical monitors. Since a measurement of beam growth due to excess energy spread depends on the subtraction of two quantities whose magnitudes are very close, large systematic errors could occur, especially in the low current regime. However, as can be seen in the following, the internal consistency of the data is good. In the analysis, Gaussian distributions are assumed and the values of $\sigma_\epsilon/\sigma_{\epsilon 0}$ are normalized to 1 at low currents.

Energy Spread (Tail)

The physical aperture of the ring is reduced by a horizontal scraper until a constant beam lifetime (usually 20 min) is reached and then the aperture is adjusted to maintain this lifetime as the current decays. As in the above, if η is known, energy spread can be extracted.[4] Care was taken to verify that no other beam enlarging effects, such as synchrobetatron resonances, interfered with the measurements; the experiments were repeated using a scraper in a position at which $\eta = 0$. The major systematic errors are introduced by distortions in the distributions of electrons due to nonlinear terms in the focusing field and imperfect knowledge of the lattice functions. Random errors are caused by spontaneous collective energy oscillations and the accuracy of the scraper.

Longitudinal Bunch Oscillation Modes

The output from a position monitor electrode, fed via 5 meters of RG/214 cable, is detected by a microwave diode and analyzed with a narrow band (100 Hz) low frequency wave analyzer. The signal is filtered in front of the diode by high and low pass filters in the 0.5 to 6 GHz region, allowing the strength of each mode to be measured as a function of its coupling frequency in the microwave range. Although signals are detected above 6 GHz it is not possible to be completely quantitative about the relative strength of the modes because the exact response characteristic of the antenna system is not known. However, the occurrence of the modes as a function of beam current can be clearly seen and changes in line widths and frequencies can be measured without a complete knowledge of the antenna system.

Energy Loss to Parasitic Modes

Using instrumentation described in Ref. 5, the shift in synchronous phase angle ϕ is measured as a function of current I by comparing signals from the beam and from an RF cavity using a hp-8405A vector voltmeter. Only relative phase change can be measured directly; absolute phase is obtained by extrapolating the plots to zero current where the synchronous phase is classically known. The parasitic mode resistance $R(\sigma_z)$ is extracted using the relation $\cos\phi = (U_0 + IR)/V$ in which U_0 is the synchrotron radiation loss per turn and V the peak cavity voltage.

*Work supported by the Energy Research and Development Administration.
†On leave from the University of Saskatchewan, Saskatoon, Canada.
††On leave from CERN, Geneva, Switzerland.

(Presented at the 1977 Particle Accelerator Conference, Chicago, Illinois. March 16 - 18, 1977)

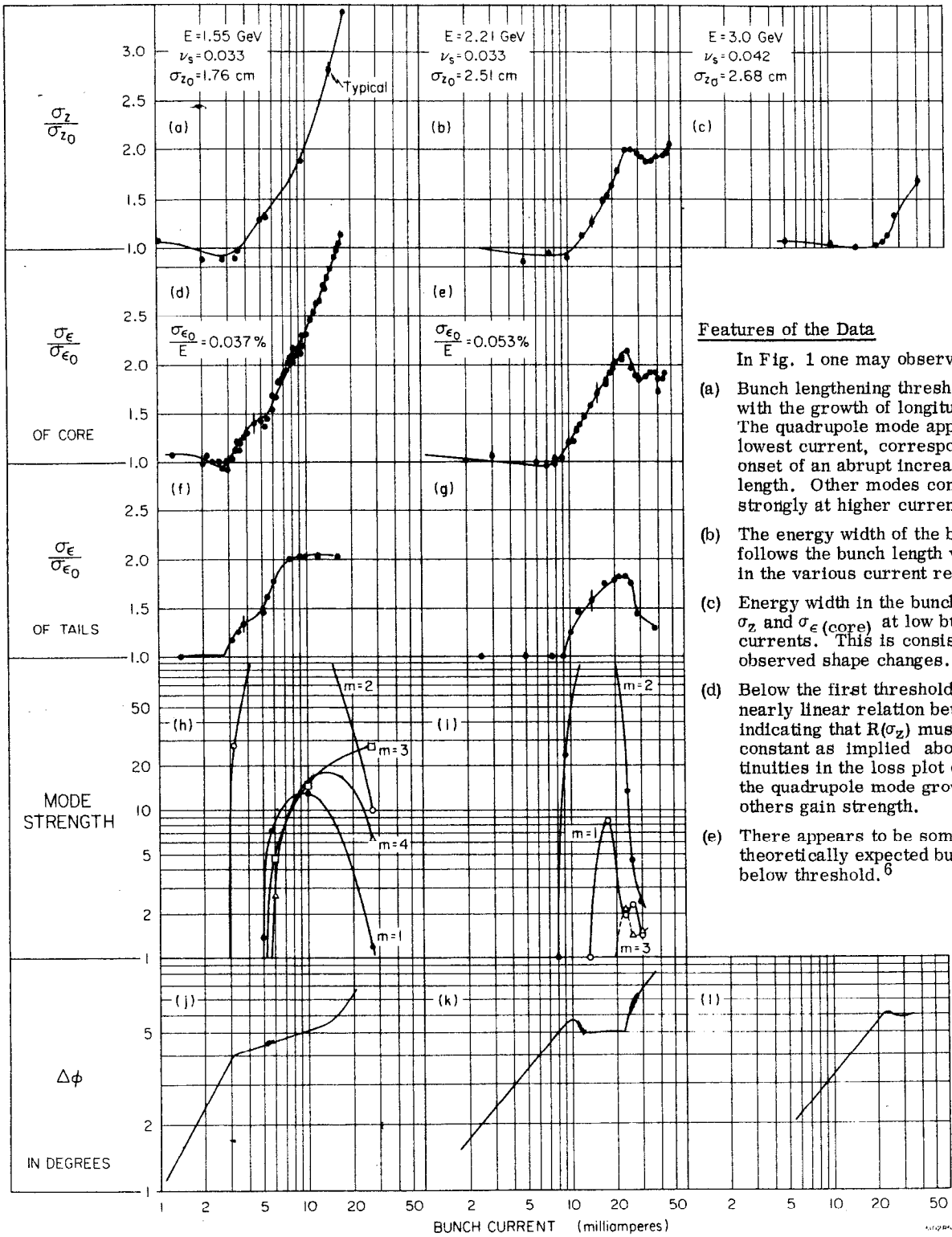

Fig. 1. Bunch length, energy spread, mode strength and phase-shift data.

Features of the Data

In Fig. 1 one may observe the following:

(a) Bunch lengthening thresholds coincide with the growth of longitudinal modes. The quadrupole mode appears at the lowest current, corresponding to the onset of an abrupt increase in bunch length. Other modes contribute less strongly at higher currents.

(b) The energy width of the bunch core follows the bunch length very closely in the various current regimes.

(c) Energy width in the bunch tails follows σ_z and σ_ϵ (core) at low but not at high currents. This is consistent with observed shape changes.

(d) Below the first threshold there is a nearly linear relation between ϕ and I indicating that $R(\sigma_z)$ must be almost constant as implied above. Discontinuities in the loss plot occur where the quadrupole mode grows or dies and others gain strength.

(e) There appears to be some evidence of theoretically expected bunch shortening below threshold.[6]

Theoretical Interpretation

Mechanism

Two types of bunch lengthening theories have already been proposed: The potential-well distortion model,[6,7] and the instability model.[8,9,10,11] The data suggest strongly that the dominant lengthening mechanism in SPEAR II results from bunch instabilities. These instabilities appear to be bounded by growth in bunch length.

Furthermore, the growth rate of this instability seems to be much greater than the synchrotron radiation damping rate. This allows us to simplify the theoretical treatment by using the Vlasov equation[12] instead of the Fokker-Planck equation.[10]

In Ref. 13, a general scaling law for bunch length σ_z is derived, relying only on the above assumptions. In a given storage ring, σ_z satisfies the scaling property $\sigma_z = F(\xi)$, where

$$\xi = \frac{I\alpha}{\nu_s^2 E} \quad .$$

(I is the beam intensity, α the momentum compaction factor, ν_s the synchrotron wave number, E the energy.)

In particular, assuming a power law behavior of the coupling impedance responsible for the instability

$$\frac{Z(\omega)}{2\pi R} = Z_0 \omega^a$$

one obtains

$$\sigma_z \propto \left(\xi Z_0 R^3\right)^{1/(2+a)} \quad .$$

This is valid for any machine of radius R and impedance parameter Z_0. In Fig. 2(a), ξ has been plotted as a function of σ_z for a fixed α. The scaling is obvious, and the slope of the fitting line indicates that in SPEAR II a = -0.68, which means that in the frequency range of interest, f > a few GHz, $Z(\omega) \propto \omega^{-0.68}$ is a slowly decreasing function of ω. The data is well parametrized by

$$\sigma_z(\text{cm}) = 5.6 \times 10^{-2} \left(\frac{I(\text{mA})\alpha}{\nu_s^2 E\,(\text{GeV})}\right)^{1/1.32}$$

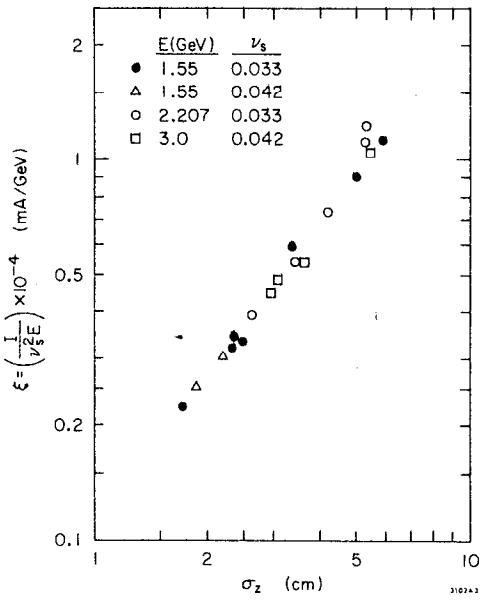

Fig. 2(a). Scaling parameter $\xi = (I/E\nu_s^2)$ as a function of σ_z.

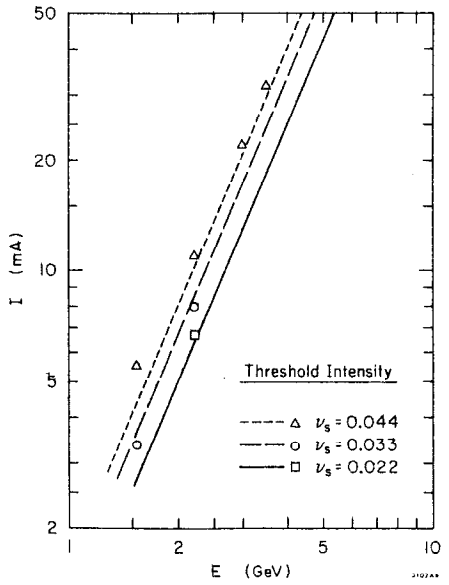

Fig. 2(b). Scaling behavior of the threshold current.

Using these results, and equating σ_z to the natural unperturbed bunch length σ_{z0}, threshold can be predicted for any set of machine parameters: For SPEAR II, $I_{th} = 13.5\ E\,(\text{GeV})\ 2.32\nu_s^{0.68}$. The observed thresholds fit this formula within a 10% error. See Fig. 2(b).

Notice that the previously used scaling law,[9] $\sigma_z \propto I^{1/3}$, assumes a $Z(\omega) \propto \omega$ dependence (a=+1). This is, however, not a bad assumption for very long bunches where Fourier components cut off around 0.5 GHz, as in SPEAR I.[1]

More can be understood about the coupling impedance responsible for the instabilities by looking at the mode behavior displayed on Fig. 1(h, i). Following Ref. 12, we define the normal mode particle densities $\rho_m(z)$ (m=1: dipole, m=2: quadrupole, etc.) and their Fourier transforms $\tilde{\rho}_m(\omega)$. The driving term of the instability is proportional to an integral over ω involving products of $Z(\omega)$ and $\tilde{\rho}_m(\omega)$.[12,13] In the case of Fig. 1(h) near threshold, $\tilde{\rho}_2$ has its maximum at 4.2 GHz (σ_z = 1.7 cm), and in this region one finds $Z \propto \omega^{-0.68}$. At high current, the bunch has lengthened (σ_z = 6.6 cm) and $\tilde{\rho}_2$ now has its maximum at 1 GHz, whereas modes 3 and 5 peak at 1.25 and 1.6 GHz, respectively. These considerations, together with the behavior of modes as displayed in Fig. 1(h), suggest that $Z(\omega)$ has a maximum around 1.3 GHz and drops abruptly at lower frequencies, as sketched on Fig. 3. A similar curve has been measured at the CERN PS for the transverse coupling impedance.[14]

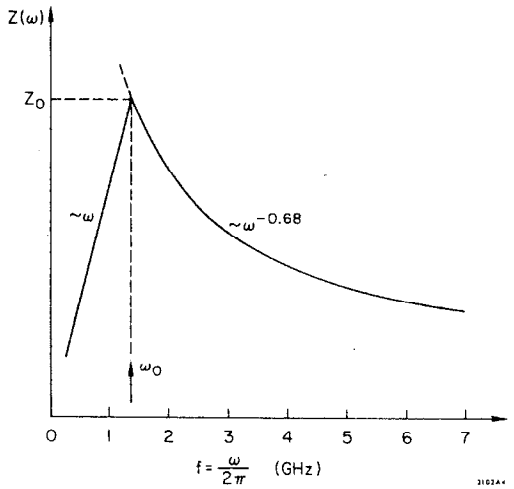

Fig. 3. Assumed form of the impedance function $Z(\omega)$ vs. ω.

Fit to the Impedance Function

The loss parameter $k(\sigma_z) = R(\sigma_z)/T_0$ (where T_0 is the revolution time) measured from runs with widely differing parameters is plotted as a function of σ_z in Fig. 4. Note that all the points fall closely on a straight line with a slope of -1.21 indicating that systematic errors in the vector voltmeter resulting from current dependent effects cannot be large. Some of the $d\phi/dI$ data (open circles) could be too high (up to 10%) because of slight bunch shortening below threshold.

The loss parameter is related to the real part of the impedance function defined as $Z(\omega)$. Assuming a Gaussian bunch

$$k(\sigma) = \frac{2}{Q^2}\int_0^\infty Z(\omega)\,I^2(\omega)\,d\omega = \frac{1}{\pi}\int_0^\infty Z(\omega)\,e^{-\omega^2\sigma^2}\,d\omega\ .$$

By using the form of $Z(\omega)$ sketched in Fig. 3 and computing $k(\sigma_z)$ from the above for various values of ω_0, theoretical plots can be obtained which can be compared with the measured data in Fig. 4. Details are described in Ref. 15. The best fit to the measured slope is obtained for $f_0 = \omega_0/2\pi = 1.3$ GHz. The magnitude is fit by $Z_0 = 9000\Omega$. This impedance is approximately equivalent to the total loss (fundamental plus higher modes) in 100 RF cells. Thus, as was inferred previously in Ref. 5, most of the loss in SPEAR II is caused by vacuum chamber components outside the 20 cell RF system.

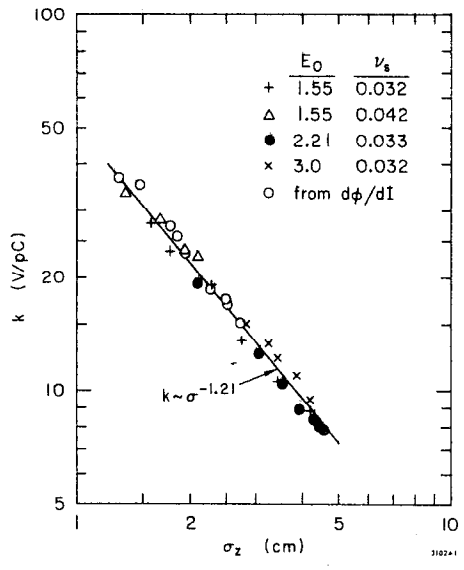

Fig. 4. The loss parameter $k(\sigma_z)$ as a function of σ_z.

Conclusions

Through simultaneous measurements of five separate aspects of bunch behavior in SPEAR II, a quantitative self-consistent picture begins to emerge. The vacuum chamber structure of the ring presents a broadband longitudinal impedance to the beam which rises as a function of frequency, attains a maximum around 1.3 GHz and then falls off as $\omega^{-0.68}$. Such an impedance is not unlike that expected for a series of low Q cavity resonators with beam ports. This impedance drives longitudinal instabilities that have thresholds and that stabilize themselves through bunch lengthening. Although the details of mode excitation are complex, it is possible to characterize bunch lengthening and broadening in such a regime by a simple scaling parameter. Finally, measurements of the bunch tails show that anomalous energy spread must be considered in the design of the apertures of future machines.

Acknowledgments

We gratefully acknowledge the help of all the other members of the SPEAR machine physics and operations groups, in particular, P. Morton and J. Paterson.

References

1. M. A. Allen et al., Proceedings of the IXth International Conference on High Energy Accelerators, Stanford Linear Accelerator Center, 1974, p. 352.
2. M. Sands, Physics with Intersecting Storage Rings, ed. B. Touschek (Academic Press, New York, 1971), p. 257 or Report No. SLAC-121, p. 129, Stanford Linear Accelerator Center (1970).
3. A. P. Sabersky, IEEE Trans. Nucl. Sci. NS-20, 638 (1973).
4. A. W. Chao, these proceedings.
5. M. A. Allen, J. M. Paterson, J. R. Rees and P. B. Wilson, IEEE Trans. Nucl. Sci. NS-22, No. 3, 1838 (1975).
6. K. L. F. Bane and P. B. Wilson, these proceedings.
7. See, for example, C. Pellegrini and A. M. Sessler, Nuovo Cimento 3A, 116 (1971).
   A. Papiernik, M. Chatard-Moulin and B. Jecko, Proceedings of the IXth International Conference on High Energy Accelerators, Stanford Linear Accelerator Center, 1974, p. 375.
   P. Germain and H. G. Hereward, CERN/MPS/DL 75-5 (1975) (unpublished).
   E. Keil, "Bunch Lengthening and Bucket Distortion due to Cavities," PEP-126, Stanford Linear Accelerator Center (1975) (unpublished).
8. A. M. Sessler, "Strongly Turbulent Collective Motion and the Anomalous Size of Stored Particle Beams," PEP-28, Stanford Linear Accelerator Center (1973) (unpublished).
9. P. Channell, "Strong Turbulence and Anomalous Length of Stored Particle Beams," Ph.D. Thesis LBL-4433 (1975) or LBL-4613 (1975) (unpublished).
10. A. Renieri, "Turbulence and Bunch Lengthening in Electron-Positron Storage Rings," LNF-76111(R), Frascati (unpublished).
11. E. Messerschmid and M. Month, "Theory for the Fast Blowup of Particle Bunches in Accelerators," BNL Report 21891 (submitted to Nucl. Instr. and Meth.). See also BNL Report 50587 and PEP-227/SPEAR-198 (1976).
12. F. Sacherer, "Methods for Computing Bunched Beam Instabilities," CERN/SI-BR/72-5.
13. A. W. Chao and J. Gareyte, "Scaling Law for Bunch Lengthening in SPEAR II," SPEAR-197/PEP-224, Stanford Linear Accelerator Center (1976) (unpublished).
14. J. Gareyte, CERN Internal Note PD/DL Note 76-10 (unpublished).
15. P. Wilson, PEP-233, Stanford Linear Accelerator Center (1977) (unpublished).